

## Accepted Manuscript

Design, synthesis and biological evaluation of novel Benzo- $\alpha$ -pyrone containing piperazine derivatives as potential BRAF<sup>V600E</sup> inhibitors

Long-Wang Chen, Ze-Feng Wang, Bo Zhu, Ruo-Jun Man, Yan-Dong Liu, Yuan-Heng Zhang, Bao-Zhong Wang, Zhong-Chang Wang, Hai-Liang Zhu

PII: S0960-894X(16)30933-7  
DOI: <http://dx.doi.org/10.1016/j.bmcl.2016.09.003>  
Reference: BMCL 24227

To appear in: *Bioorganic & Medicinal Chemistry Letters*

Received Date: 1 June 2016  
Revised Date: 13 August 2016  
Accepted Date: 2 September 2016

Please cite this article as: Chen, L-W., Wang, Z-F., Zhu, B., Man, R-J., Liu, Y-D., Zhang, Y-H., Wang, B-Z., Wang, Z-C., Zhu, H-L., Design, synthesis and biological evaluation of novel Benzo- $\alpha$ -pyrone containing piperazine derivatives as potential BRAF<sup>V600E</sup> inhibitors, *Bioorganic & Medicinal Chemistry Letters* (2016), doi: <http://dx.doi.org/10.1016/j.bmcl.2016.09.003>

This is a PDF file of an unedited manuscript that has been accepted for publication. As a service to our customers we are providing this early version of the manuscript. The manuscript will undergo copyediting, typesetting, and review of the resulting proof before it is published in its final form. Please note that during the production process errors may be discovered which could affect the content, and all legal disclaimers that apply to the journal pertain.



**Design, synthesis and biological evaluation of novel  
Benzo- $\alpha$ -pyrone containing piperazine derivatives as  
potential BRAF<sup>V600E</sup> inhibitors**

**Long-Wang Chen<sup>a†</sup>, Ze-Feng Wang<sup>a†</sup>, Bo Zhu<sup>b</sup>, Ruo-Jun Man<sup>a</sup>, Yan-Dong Liu<sup>a</sup>,  
Yuan-Heng Zhang<sup>a</sup>, Bao-Zhong Wang<sup>a\*</sup>, Zhong-Chang Wang<sup>a\*</sup>, Hai-Liang  
Zhu<sup>a\*</sup>**

*<sup>a</sup> State Key Laboratory of Pharmaceutical Biotechnology, Nanjing University,*

*Nanjing 210023, People's Republic of China*

*<sup>b</sup> Jiangsu Chia Tai Tianqing Pharmaceutical Co., Ltd. Nanjing 210000, P. R. China*

\*Corresponding author. Tel. & fax: +86-25-89682572; e-mail: [zhuhl@nju.edu.cn](mailto:zhuhl@nju.edu.cn)

†These two authors equally contributed to this paper.

**Abstract**

The increasingly acquired resistance to vemurafenib and side effects of known inhibitors motivate the search for new and more effective anti-melanoma drugs. In this report, virtual screening and scaffold growth were combined together to achieve new molecules as BRAF<sup>V600E</sup> inhibitors. Along with docking simulation, a primary screen *in vitro* was performed to filter the modifications for the lead compound, which was then substituted, synthesized and evaluated for their inhibitory activity against BRAF<sup>V600E</sup> and several melanoma cell lines. Out of the obtained compounds, derivative **31** was identified as a potent BRAF<sup>V600E</sup> inhibitor and exerted an anticancer effect through BRAF<sup>V600E</sup> inhibition. The following biological evaluation assays confirmed that **31** could induce cell apoptosis and marked DNA fragmentation. Furthermore, **31** could arrest the cell cycle at the G0/G1 phase in melanoma cells. The docking simulation displayed that **31** could tightly bind with the crystal structure of BRAF<sup>V600E</sup> at the active site. Overall, the biological profile of **31** suggests that this compound may be developed as a potential anticancer agent.

**Key words:**

Melanoma; BRAF<sup>V600E</sup>; Virtual screening; Benzo- $\alpha$ -pyrone; Docking simulation

The RAS/RAF/MEK/ERK (MAPK) signaling pathway which could be widely activated in cells<sup>1</sup> plays a crucial role in transducing extracellular signals into the nucleus through receptor tyrosine kinases<sup>2</sup> and it has been associated to the regulation of cell proliferation, differentiation, survival and migration.<sup>3,4</sup> It is commonly accepted that RAF kinases (ARAF, BRAF and CRAF), the key components of the MAPK signaling pathway, act downstream of RAS and are in charge of MEK and ERK activation.<sup>5</sup> The abnormal activation of RAF, generally BRAF, gives rise to amplification of the MAPK pathway and is frequently observed in human cancers and contributes to oncogenesis.<sup>6</sup> Pathological studies have reported that activated forms of the BRAF gene present in approximately 8% of all cancers<sup>7</sup> and are most frequently associated with melanoma.<sup>8</sup> In detail, mutated BRAF is featured in 82% of cutaneous melanocyte nevi,<sup>9</sup> 66% of primary melanomas<sup>10</sup> and 40-68% of metastatic melanomas.<sup>11</sup> What is noteworthy is that more than 90% of the detected BRAF mutations are V600E mutated, which increases the kinase activity dramatically and concomitantly activates the signaling at relatively high levels.<sup>12</sup> Generally, the success of novel cancer therapies depends on the identification of functional targets that are essential of tumor growth and survival.<sup>13</sup> In this regard, BRAF<sup>V600E</sup> has been an attractive target for therapeutic intervention targeting which has proved to be a major advancement in the field of melanoma treatment.

To date, numbers of inhibitors against BRAF<sup>V600E</sup> have been developed and more are at various stages of preclinical and clinical development.<sup>14,15</sup> It is heartening to see vemurafenib (PLX4032), GSK2118436 and so on, selective inhibitors of BRAF<sup>V600E</sup>,

have exhibited remarkable clinical activity in patients with melanoma. Especially, vemurafenib, a 7-azaindole derivative, has received FDA approval for the treatment of late stage metastatic melanoma.<sup>16</sup> Notwithstanding these achievements, many cases of acquired resistance to vemurafenib<sup>17,18</sup> and high incidences (around 25%) of keratoacanthoma and squamous cell carcinomas associated with known inhibitors<sup>19,20</sup> have been reported in latest studies. In addition, what should be noticed is that the incidence of melanoma has greatly increased over the past decade.<sup>21,22</sup> Therefore, to break these limitations of vemurafenib and some other drugs, the development of novel potent BRAF<sup>V600E</sup> inhibitors is significantly important.

High-throughput virtual screening, which is now widely used in pharmaceutical research, is a screening method frequently used by medicinal chemists. The availability of a high-resolution crystal structure of the protein target as a template for computational screening promotes the feasibility of virtual screening.<sup>12,23</sup> The availability of the crystal structure of the BRAF<sup>V600E</sup> protein kinase now provides an opportunity for utilizing the virtual screening strategy to identify BRAF<sup>V600E</sup> inhibitors. To find more potent compounds with novel scaffolds toward BRAF<sup>V600E</sup>, a hierarchical virtual screening process was initiated. In this study, about 20,000 theoretically lead-like small molecules were randomly selected from the ZINC database firstly. The compounds were then docked into the ATP-binding site of the BRAF<sup>V600E</sup> kinase (PDB code: 2FB8) using the LibDock module in Discovery Studio (version 3.5). After virtual screening combined with scaffold growth, the new grown molecules were ranked according to the binding modes and binding affinity. The best

ones were selected to be synthesized subsequently, whereafter the best entity **3a** (Fig. 1) was picked out from the preliminary test and chosen as a lead compound. Derivatives of this compound (**3a**) were thereafter synthesized and evaluated by additional bioassays depicting their pharmacological profile.

Herein, we reported a series of BRAF<sup>V600E</sup> inhibitors bearing the benzo- $\alpha$ -pyrone scaffold and emphasized the rationale behind the discovery of inhibitors, the study of structure-activity relationship, mechanisms of inhibition and the effect of the inhibitors on the viability of melanoma cells.

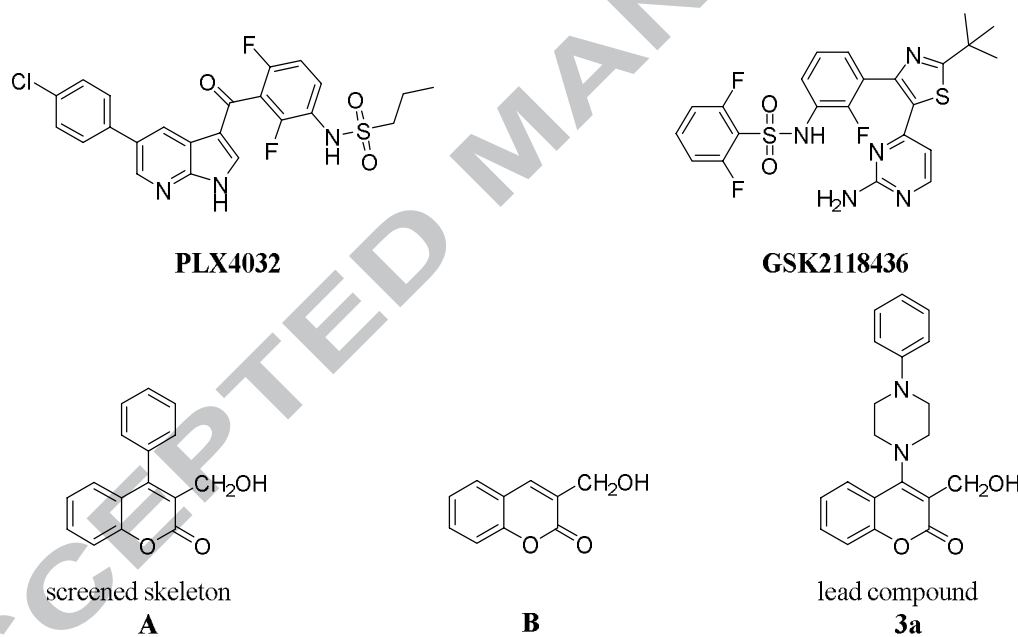
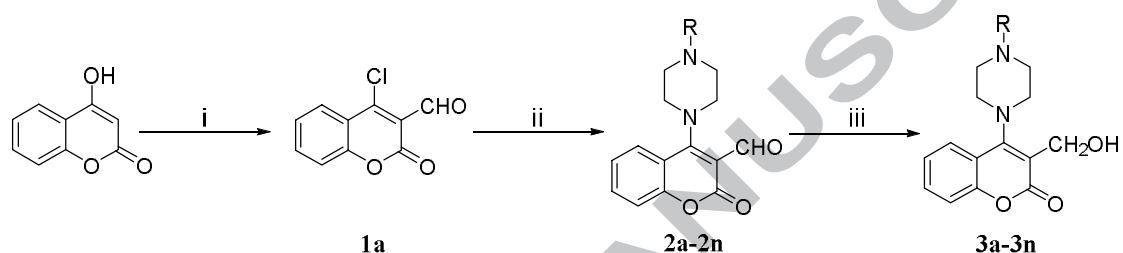


**Fig. 1.** Chemical structures of known BRAF<sup>V600E</sup> inhibitors and designed structures.

The synthesis of compounds **3a-3n** followed the general pathway depicted in **Scheme 1<sup>a</sup>**. All the target compounds were obtained in three steps as described in the supplementary experimental section, the reactions were monitored by thin layer chromatography (TLC), and the crude products were purified by column chromatography. All of the synthetic compounds **3a-3n** were reported for the first

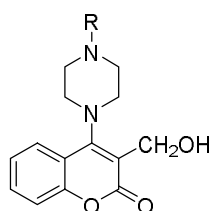
time (**Table 1**) and gave satisfactory analytical and spectroscopic data, i.e.  $^1\text{H}$  NMR, EI-MS, which were in accordance with the assigned structures. Furthermore, the crystal structure of compound **3f** (CCDC No. 1471892) was determined by single crystal X-ray diffraction analysis in **Fig. 2**, and its crystal data, data collection and refinement parameters were listed in **Table S1**.

**Scheme 1<sup>a</sup>**.



<sup>a</sup>: The synthetic routes of compounds **3a-3n**. Reagents and conditions: (i) Phosphorus oxychloride, Dimethyl formamide, 65 °C, 5 h; (ii) Different substituted piperazine,  $\text{K}_2\text{CO}_3$ , Dichloromethane, 0 °C, 0.5 h; (iii) Sodium borohydride, anhydrous ethanol, 0 °C, 3 h.

**Table 1.** Structures of compounds **3a-3n**.



Compounds	R	Compounds	R
<b>3a</b>		<b>3h</b>	
<b>3b</b>	$-\text{CH}_2\text{CH}_3$	<b>3i</b>	
<b>3c</b>		<b>3j</b>	

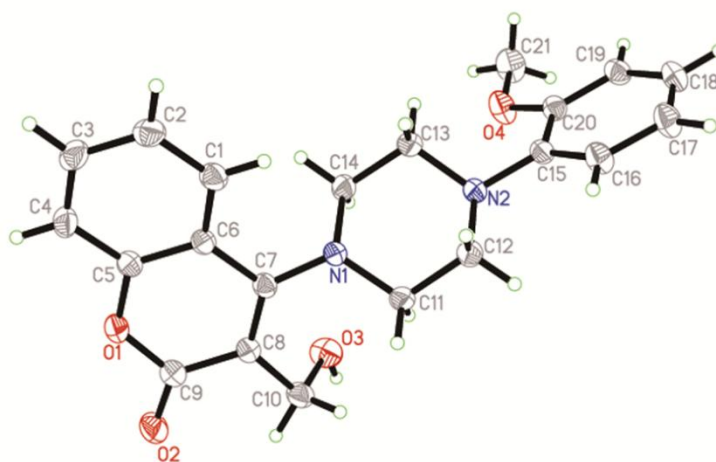
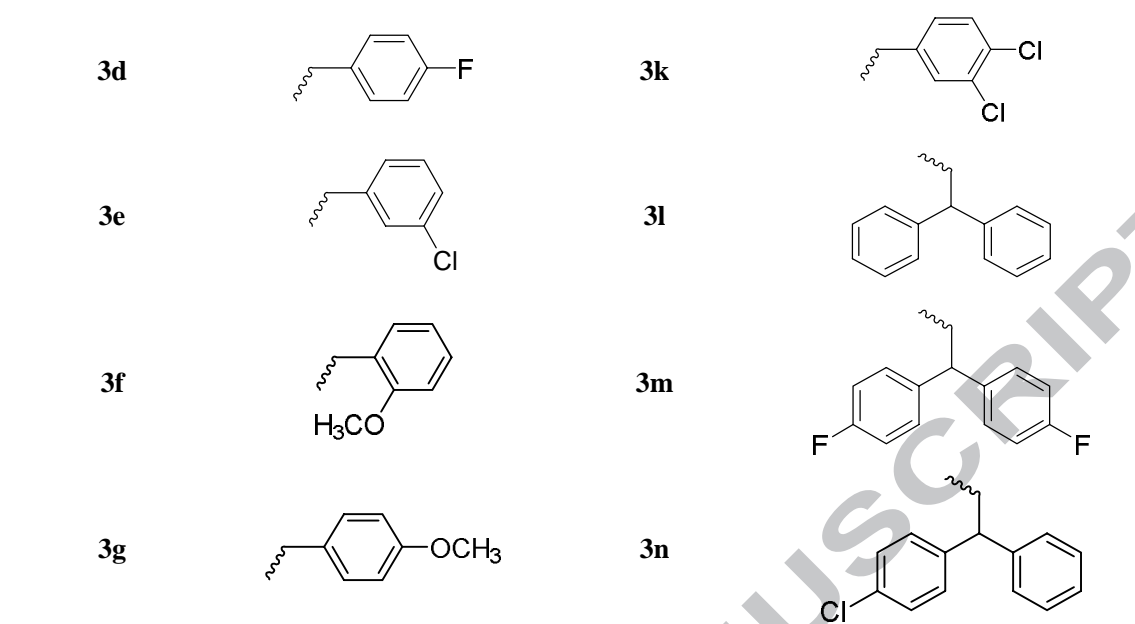


**Fig. 2.** Crystal structure diagram of compound **3f**.

To evaluate the antiproliferative activities of the prepared compounds, the BRAF<sup>WT</sup> melanoma cells (WM1361), BRAF<sup>V600E</sup> melanoma cells (WM266-4) and human skin melanoma cells (A375) were used and the results were summarized in **Table 2**. Out of all the compounds, compound **3l** possesses an excellent antiproliferative activity specifically for A375 and WM266-4 (BRAF<sup>V600E</sup>) cell lines,

with  $IC_{50}$  values of 2.24  $\mu$ M and 1.35  $\mu$ M, compared to the positive control vemurafenib which showed better inhibitory potential for A375 and WM266-4 ( $IC_{50}$  = 0.21  $\mu$ M and  $IC_{50}$  = 0.07  $\mu$ M), while compound **3l** exhibited relatively worse inhibitory activity against WM1361 (wild type BRAF) cell line ( $IC_{50}$  = 21.08  $\mu$ M). Moreover, for most compounds, there was no or negligible effects were observed for the WM1361 (wild type BRAF) cell line even when treated with doses as high as 50  $\mu$ M although they could mildly inhibit BRAF<sup>V600E</sup> cell lines to some extent. These data demonstrated that the compounds were able to induce cytotoxicity selectively in the BRAF mutated melanoma cancerous cells.

**Table 2** *In vitro* inhibitory effects of compounds **3** (**3a-3n**) against human tumor cell lines, normal cell line.

Compounds	$IC_{50} \pm SD$ ( $\mu$ M)			$CC_{50} \pm SD$ ( $\mu$ M)
	A375 <sup>a</sup>	WM-266-4 <sup>a</sup>	WM1361 <sup>a</sup>	293T <sup>b</sup>
<b>3a</b>	17.25 $\pm$ 0.33	16.55 $\pm$ 0.57	> 50	> 50
<b>3b</b>	> 50	> 50	> 100	> 50
<b>3c</b>	32.09 $\pm$ 0.28	37.64 $\pm$ 0.19	> 50	> 50
<b>3d</b>	24.72 $\pm$ 0.34	23.35 $\pm$ 0.25	> 50	> 50
<b>3e</b>	40.45 $\pm$ 0.53	46.33 $\pm$ 0.36	> 50	> 50
<b>3f</b>	19.96 $\pm$ 0.47	18.34 $\pm$ 0.45	> 50	> 50
<b>3g</b>	7.23 $\pm$ 0.21	5.61 $\pm$ 0.17	40.36 $\pm$ 0.24	> 50
<b>3h</b>	6.51 $\pm$ 0.36	5.33 $\pm$ 0.22	38.09 $\pm$ 0.38	> 50
<b>3i</b>	31.94 $\pm$ 0.31	30.04 $\pm$ 0.43	> 50	> 50
<b>3j</b>	8.45 $\pm$ 0.25	6.56 $\pm$ 0.16	45.88 $\pm$ 0.44	> 50
<b>3k</b>	7.66 $\pm$ 0.63	6.04 $\pm$ 0.42	42.72 $\pm$ 0.33	> 50
<b>3l</b>	2.24 $\pm$ 0.15	1.35 $\pm$ 0.17	21.08 $\pm$ 0.54	> 50
<b>3m</b>	3.16 $\pm$ 0.32	2.57 $\pm$ 0.14	29.41 $\pm$ 0.26	> 50
<b>3n</b>	3.89 $\pm$ 0.17	2.74 $\pm$ 0.21	30.15 $\pm$ 0.24	> 50
<b>Vemurafenib</b> <sup>c</sup>	0.21 $\pm$ 0.02	0.07 $\pm$ 0.01	1.86 $\pm$ 0.12	> 50

<sup>a</sup> Inhibition of the growth of tumor cell lines

<sup>b</sup> Inhibition of the growth of normal cell line

<sup>c</sup> Used as positive control

Subsequently, all the synthetic compounds **3a-3n** were evaluated for inhibitory

activity against the BRAF<sup>V600E</sup> enzyme to obtain a further understanding of the structure-activity relationships (SAR) and the results were presented in **Table 3**. From the data listed, it can be found that compound **3b** of which piperazine connected to an alkane substituent showed the worst inhibitory activity ( $IC_{50} > 50 \mu M$ ). In comparison with **3b**, aromatic-substituted compounds were more potent, indicating that the short chain group was not conducive to BRAF<sup>V600E</sup> inhibition and the modification on the aryl rings seems to be beneficial to enzyme inhibition. When it comes to the phenylpiperazine, we introduced a variety of groups to enrich the diversity. Halo-substituted compounds **3c-3e** and compound **3i** with a trifluoromethyl displayed a dramatic loss in activity compared to unsubstituted analog (**3a**,  $IC_{50} = 8.93 \mu M$ ), while compounds **3g** and **3h** afforded about 5-fold improvement over the compound **3a**, which suggested that substituent groups can affect the inhibitory activities and compounds with electron-donating groups exhibited better inhibitory activities than those with electron-withdrawing groups.

Additionally, the level of BRAF inhibition was almost not altered when we changed the position of the fluoro atom from the *ortho*-position (**3c**) to the *para*-position (**3d**), and the exchange of the methoxy group from the *meta*- (**3h**) to the *para*-position (**3g**) resulted in an equal potency too. All the results demonstrated that the change of substituent position may not have much effect on the inhibitory activity. In the case of compounds (**3e**, **3j** and **3k**) with chlorine groups on phenyl ring, compounds **3j** and **3k** which were introduced two chlorine atoms at 2,3-position or 3,4-position on phenyl ring, exhibited over 10-fold greater advantages than compound

**3e**. Besides, compounds (**3l-3n**) which have a benzhydryl group exhibited a significant increment in activity comparing to other compounds. Among them, compound **3l**, possessed the most potent BRAF<sup>V600E</sup> inhibitory activity with IC<sub>50</sub> of 0.37  $\mu$ M. In a word, the new class of compounds furnished several antagonists of BRAF<sup>V600E</sup> which have potential development value for further exploration.

**Table 3.** Inhibition activity of all tested compounds against BRAF<sup>V600E</sup>.

Compounds	IC <sub>50</sub> $\pm$ SD ( $\mu$ M)	Compounds	IC <sub>50</sub> $\pm$ SD ( $\mu$ M)
	BRAF <sup>V600E</sup>		BRAF <sup>V600E</sup>
<b>3a</b>	8.93 $\pm$ 0.21	<b>3i</b>	24.23 $\pm$ 0.21
<b>3b</b>	> 50	<b>3j</b>	3.27 $\pm$ 0.25
<b>3c</b>	22.01 $\pm$ 0.14	<b>3k</b>	2.56 $\pm$ 0.14
<b>3d</b>	17.81 $\pm$ 0.21	<b>3l</b>	0.37 $\pm$ 0.12
<b>3e</b>	33.49 $\pm$ 0.18	<b>3m</b>	0.68 $\pm$ 0.06
<b>3f</b>	10.12 $\pm$ 0.16	<b>3n</b>	0.92 $\pm$ 0.13
<b>3g</b>	1.84 $\pm$ 0.13	<b>Vemurafenib<sup>a</sup></b>	0.04 $\pm$ 0.02
<b>3h</b>	1.76 $\pm$ 0.19		

<sup>a</sup> Used as positive control

To test whether the inhibition of cell growth of WM266-4 was related to cell apoptosis and verify further the selective cytotoxicity between WM266-4 and WM1361, two kinds of cell lines apoptosis induced by compound **3l** was determined using flow cytometry. WM266-4 cells were treated with varying concentrations (0  $\mu$ M, 2  $\mu$ M, 4  $\mu$ M and 8  $\mu$ M) of **3l** for 24 h. As shown in **Fig. 3**, the percentage of apoptotic cells was markedly increased in a dose-dependent manner after treatment with different doses of **3l**. Meanwhile, we treated WM1361 cells with 20  $\mu$ M, 40  $\mu$ M and 60  $\mu$ M of **3l** for 24 h. However, the results presented in **Fig. 4** showed that cells remained unaffected even after 24 h treatment at high doses. Combing these results together we concluded that compound **3l** can selectively cause cell apoptosis in

WM266-4 cells while wild type BRAF melanoma cells will be unaffected by this treatment.

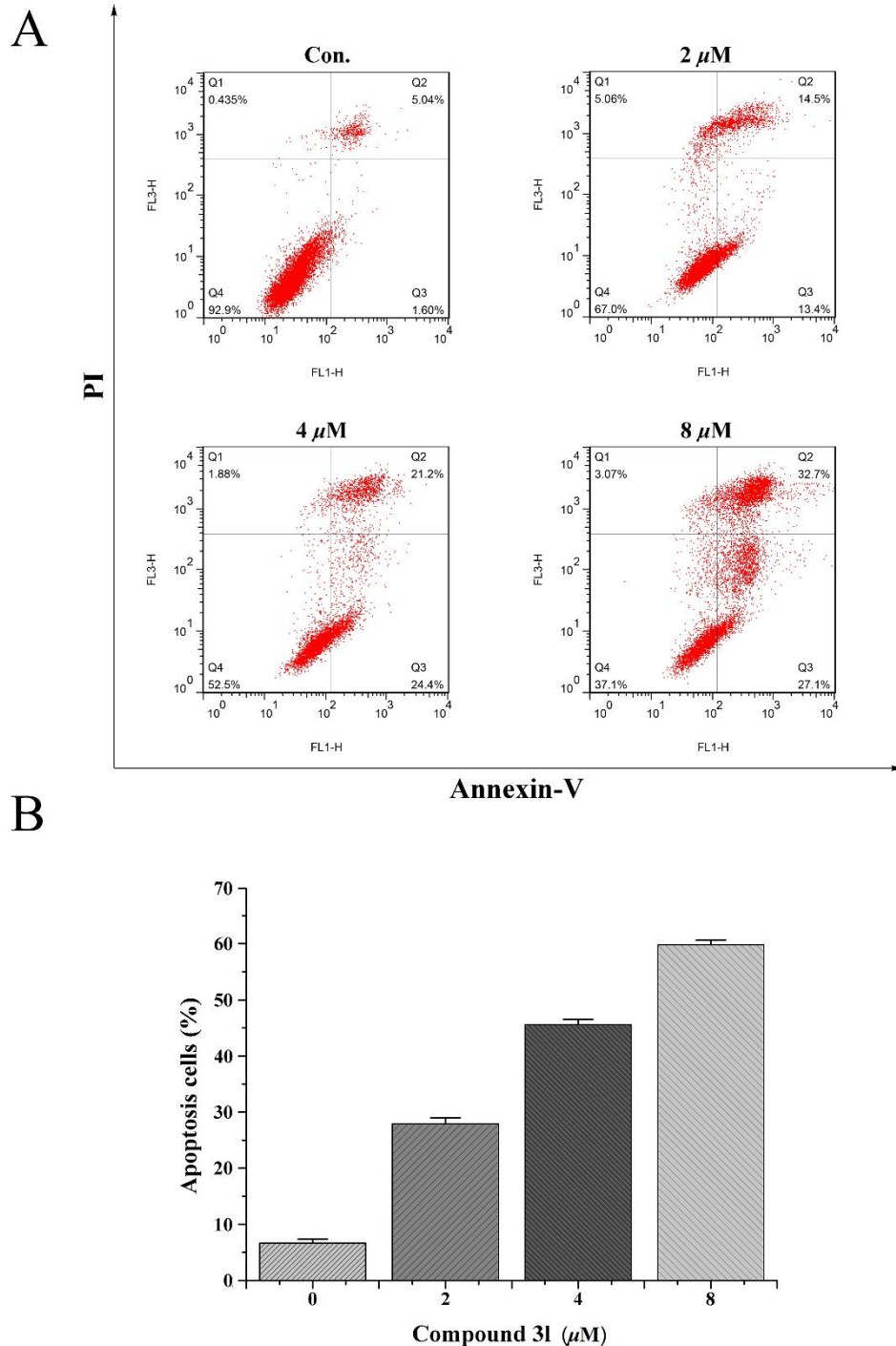


**Fig. 3.** Annexin V-FITC/PI dual-immuno-fluorescence staining after treatment with different concentrations of **31** on WM266-4 cells revealed significantly increased number of apoptotic cells. (A) The apoptosis rate of WM266-4 cells treated with 0, 2, 4 and 8  $\mu\text{M}$  **31** for 24 h. (B) The percentage of apoptotic cells were calculated after the treatment of **31**. Images are representative of

three independent experiments.

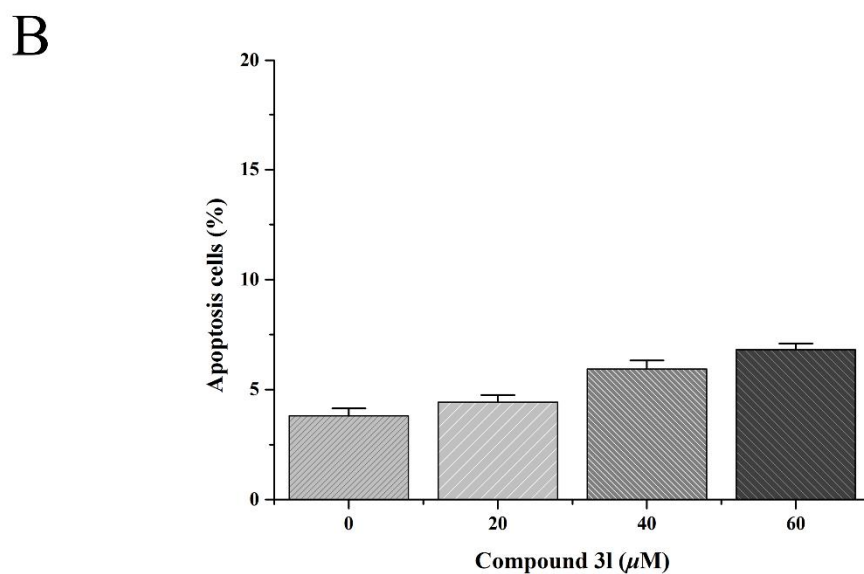
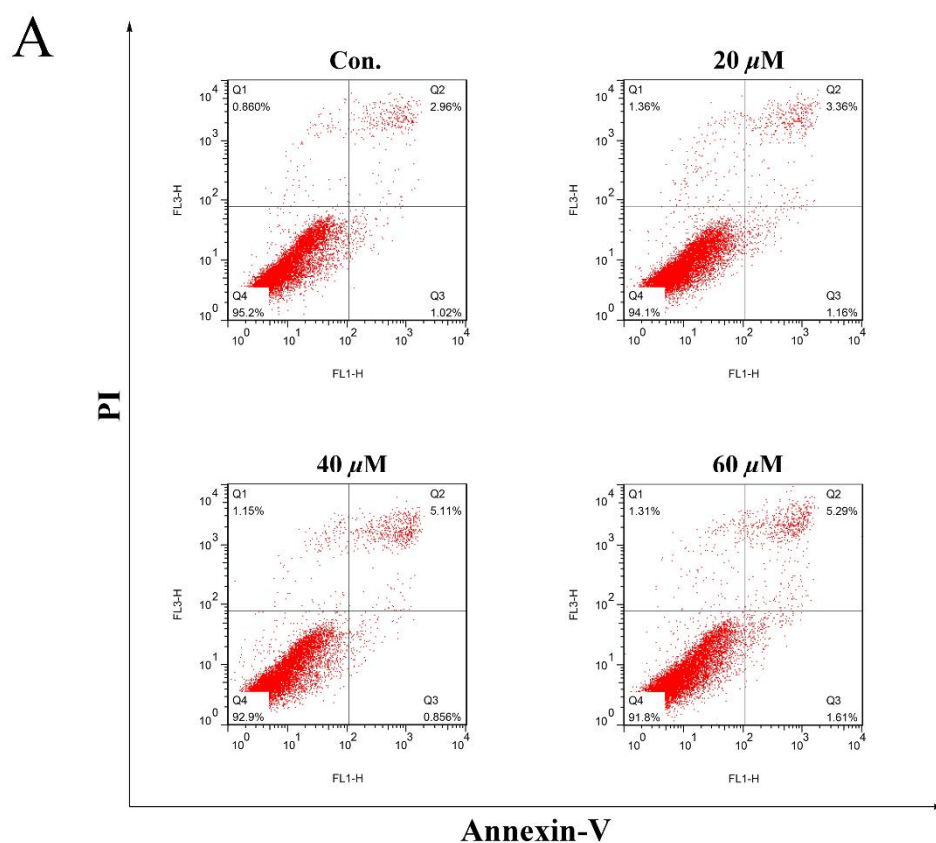


**Fig. 4.** Annexin V-FITC/PI dual-immuno-fluorescence staining after treatment with different concentrations of **31** on WM1361 cells revealed significantly increased number of apoptotic cells. (A) The apoptosis rate of WM1361 cells treated with 0, 20, 40 and 60  $\mu\text{M}$  **31** for 24 h. (B) The percentage of apoptotic cells were calculated after the treatment of **31**. Images are representative of three independent experiments.

Generally speaking, when apoptosis occurs, DNA is cleaved into internucleosomal fragments which is a late marker of apoptosis. To further confirm cell programmed death mediated by **31** in WM266-4, a DNA fragmentation assay was implemented. WM266-4 cells were cultured in the presence of the various concentrations of compound **31** (0  $\mu$ M, 2  $\mu$ M, 4  $\mu$ M and 8  $\mu$ M) for 24 h. As depicted in **Fig. 5**, compound **31** could result in marked DNA fragmentation in WM266-4, whereas the control (untreated with **31**) did not exhibit any DNA ladder.

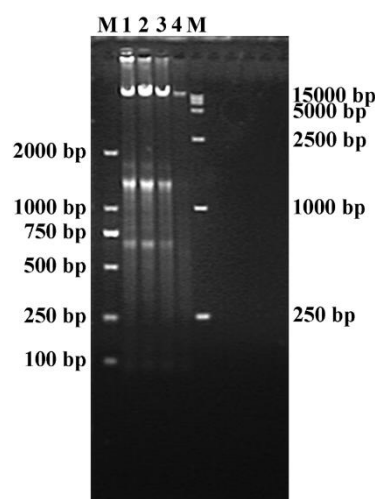


**Fig. 5.** The gel electrophoresis image obtained after DNA fragmentation assay for apoptosis detection. WM266-4 cells were cultured at 37 °C for 24 h in the presence or absence of the various concentrations of compound **31**. DNA was isolated and visualized on a 2.0% agarose gel. From left lanes are: Lane M: Marker (2000bp); Lane 1: 8  $\mu$ M; Lane 2: 4  $\mu$ M; Lane 3: 2  $\mu$ M; Lane 4: 0  $\mu$ M (CON); Lane M: Marker (15000bp).

We next assessed the cell cycle distribution of WM266-4 cells by flow cytometry. Cells treated with compound **31** of different concentrations (0, 2, 4, and 8  $\mu$ M) for 24 h (**Fig. 6**) and cells treated with 8  $\mu$ M **31** for different times (0, 12, 24, and 36 h) (**Fig. 7**) could both arrest a significant number of cells in G0/G1 phase. In summary, as shown in **Fig. 6**, the accumulation of cells in G0/G1 phase increases with increased drug

concentration. Furthermore, **Fig. 7** demonstrated that the maximum accumulation of cells in G<sub>0</sub>/G<sub>1</sub> phase was observed after treatment with 8  $\mu$ M **31** for 36 h.

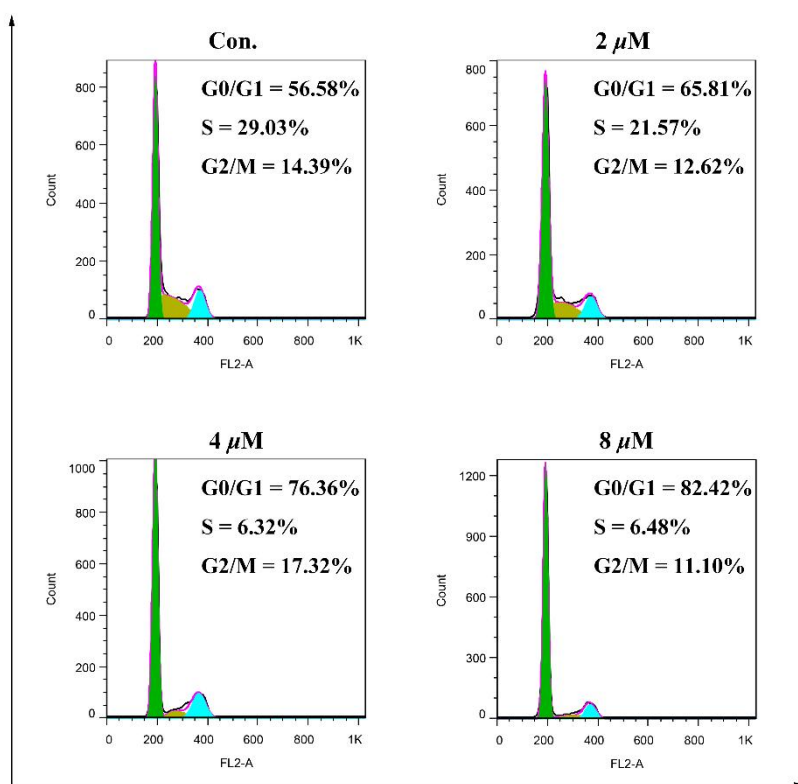


**Fig. 6.** Effect of compound **31** on the cell cycle distribution of WM266-4 cells in a dose-dependent manner (0, 2, 4 and 8  $\mu$ M). Images are representative of three independent experiments. (G<sub>1</sub> phase, green; S phase, yellow and G<sub>2</sub>/M phase, blue).

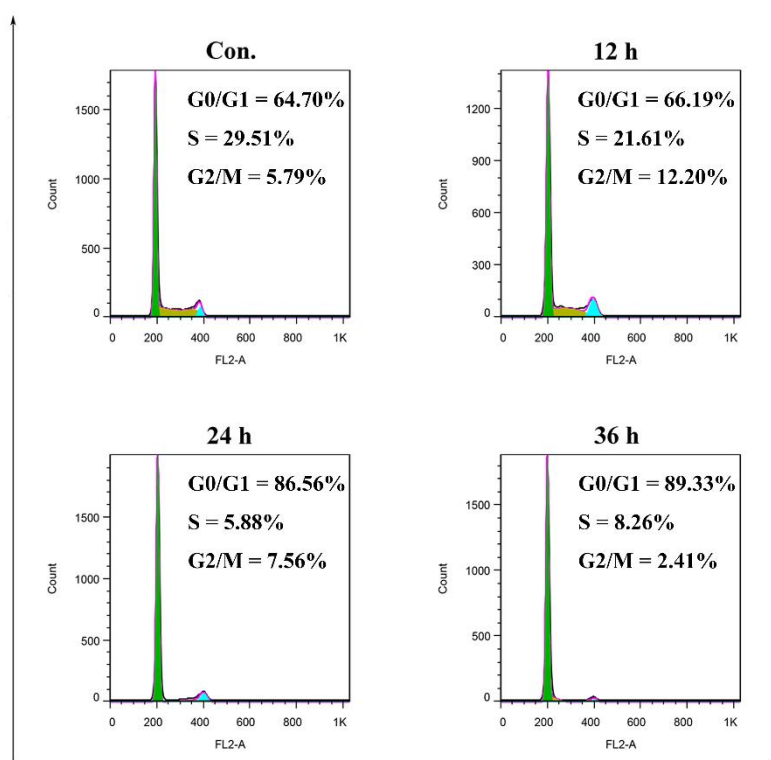


**Fig. 7.** Effect of compound **31** on the cell cycle distribution of WM266-4 cells in a time-dependent manner (0, 12, 24 and 36 h). Images are representative of three independent experiments. (G1 phase, green; S phase, yellow and G2/M phase, blue).

In order to explore potential anti-tumor agents, all the compounds were evaluated by the MTT assay for their toxicity against 293T which was defined by the median cytotoxic concentration ( $CC_{50}$ ) data. As shown in **Table 2**, most of the analogues possessed low cytotoxicity.

In this study, the docking simulation was employed repetitiously and the screened skeleton **A** (**Fig. 1**) as springboard was firstly calculated to predict the binding mode (**Fig. S1A**). As showed in picture there was still adequate margin of space to be utilized. From the perspective of strong potency, the inner side groove should be occupied to offer additional interactions and the binding potency could be enhanced if the screened skeleton can be optimized by favorable fragments.

Meanwhile, modification of the benzene ring is so limited that we removed the skeleton artificially to give structure **B** (Fig. 1). Skeleton **B** was then used as a template to grow scaffold to acquire new molecules as BRAF<sup>V600E</sup> inhibitors. In this work this process was performed automatically by the Scaffold Grow module in Discovery Studio 3.5, complemented by the docking screening. After calculating and scoring, series of new molecules were constructed and ranked and they were synthesized and initially tested. The lead compound **3a** was then validated. Modification was made to lead compound to provide chemical diversity and each of the derivatives was evaluated by bioassays.

In addition, for the purpose of giving a better understanding of the excellent activity observed, we examined the interaction of the most potent inhibitor **3l** with the BRAF<sup>V600E</sup>. The binding modes of compound **3l** and BRAF were depicted in Fig. 8 and in this binding mode, compound **3l** binded into BRAF<sup>V600E</sup> via two hydrogen bonds, one  $\pi$ -sulfur interaction and one  $\pi$ - $\pi$  stacked interaction. The oxygen atom of hydroxyl group connected with benzo- $\alpha$ -pyrone skeleton formed two hydrogen bonds with Asn581 and Asp594 residues respectively. The  $\pi$ -sulfur interaction was formed between a benzene ring of benzhydryl group and Cys532. Moreover, the benzene ring moiety of benzhydryl group is intercalated into the space to form a  $\pi$ - $\pi$  stacked interaction with residue Phe583. The receptor surface model shown in Fig. 8B revealed that **3l** with benzhydryl has a good shape complementarity with the ATP-binding pocket of BRAF and the above-mentioned three kinds of forces may contribute to afford an explanation for its nice activity. Besides, the higher binding

affinity of **31** might also be accounted for by some weak interactions, such as  $\pi$ -alkyl interaction, Van der Waals forces and others. All in all, this molecular docking result, along with the enzyme assay data, suggests that the modification suited our intention and **31** was a potential inhibitor of BRAF<sup>V600E</sup>.

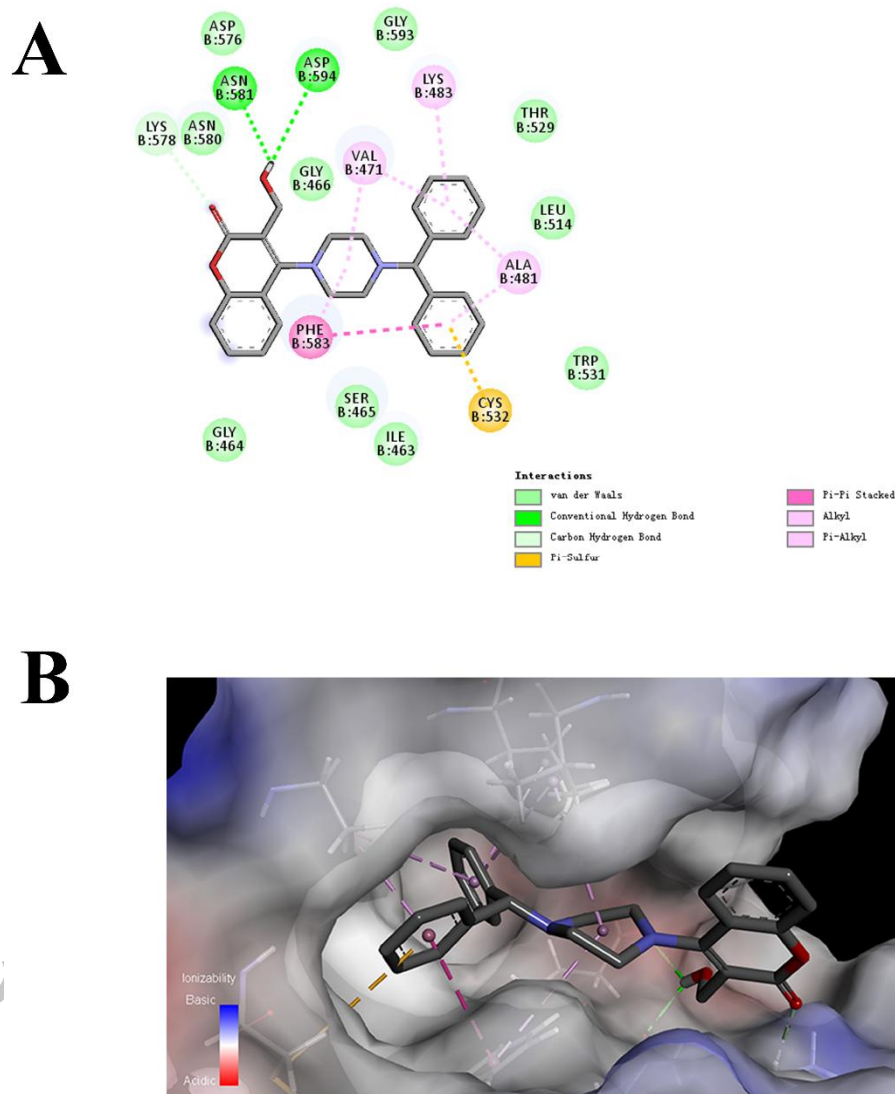


**Fig. 8.** Binding mode of compound **31** with BRAF<sup>V600E</sup> (PDB code: 2FB8). (A) 2D diagram of the interaction between compound **31** and amino acid residues of the nearby active site. (B) 3D diagram of compound **31** inserted in the BRAF<sup>V600E</sup> binding site: for clarity, only interacting residues are displayed.

The BRAF mutant, BRAF<sup>V600E</sup>, an important and interesting therapeutic target in

human melanoma and other kinds of cancer, has attracted increasing attentions of the researchers and vemurafenib was developed under this situation. However, recent clinical studies have reported the acquired resistance to vemurafenib and side effects of some other drugs in many cases. Therefore, to further explore the anti-proliferative potential of BRAF<sup>V600E</sup> inhibitors, we utilized virtual screening combined with scaffold growth to design a sequence of novel harmless benzo- $\alpha$ -pyrone-piperazine derivatives and decent activities which were tested in a series of experiments, and the results indicated that some compounds may be promising in drug development. Among them, **31** was impressive and it showed better selective cytotoxicity towards three cell lines (A375, WM266-4 and WM1361) in MTT assay in which **31** displayed better anti-proliferative activity against WM266-4 and A375 cell lines than WM1361. The BRAF<sup>V600E</sup> inhibitory assay further revealed that **31** possessed superior inhibitory potency with an IC<sub>50</sub> of 0.37  $\mu$ M. Apoptosis results confirmed that compound **31** can selectively cause cell apoptosis in WM266-4 cells while wild type BRAF cells will be unaffected by this treatment. The following DNA fragmentation assay showed **31** could be a potential pro-apoptotic agent. Additionally, compound **31** could induce cell cycle arrest in G0/G1 phase in a dose- and time-dependent manner. Molecular docking studies afforded a good understanding and explanation of **31** impressive performance. In summary, we hope these findings will benefit the study of cancer treatment through BRAF<sup>V600E</sup> inhibition.

### Acknowledgements

The work was financed by the Projects (Nos. CXY1409 & CG1305) from the

Science & Technology Bureau of Lianyungang City of Jiangsu Province.

## References and Notes

1. Wellbrock, C.; Karasaride, M.; Marais, R. *Nat. Rev. Mol. Cell Biol.* **2004**, *5*, 875.
2. Qin, J.; Xie, P.; Ventocilla, C.; Zhou, G.; Vultur, A.; Chen, Q.; Liu, Q.; Herlyn, M.; Winkler, J.; Marmorstein, R. *J. Med. Chem.* **2012**, *55*, 5220.
3. Karra, A. S.; Taylor, C. A.; Thorne, C. A.; Cobb, M. H. *Cancer cell* **2015**, *28*, 145.
4. Yang, F.; Li, J.; Zhu, J.; Wang, D.; Chen, S.; Bai, X. *Eur. J. Pharmacol.* **2015**, *754*, 105.
5. Subramanian, S.; Costales, A.; Williams, T. E.; Levine, B.; McBride, C. M.; Poon, D.; Amiri, P.; Renhowe, P. A.; Shafer, C. M.; Stuart, D. *ACS Med. Chem. Lett.* **2014**, *5*, 989.
6. Chraybi, M.; Alsamad, I. A.; Copie-Bergman, C.; Baia, M.; André, J.; Dumaz, N.; Ortonne, N. *Hum. Pathol.* **2013**, *44*, 1902.
7. Holderfield, M.; Deuker, M. M.; McCormick, F.; McMahon, M. *Nat. Rev. Cancer* **2014**, *14*, 455.
8. Villanueva, J.; Vultur, A.; Lee, J. T.; Somasundaram, R.; Fukunaga-Kalabis, M.; Cipolla, A. K.; Wubbenhorst, B.; Xu, X.; Gimotty, P. A.; Kee, D. *Cancer cell* **2010**, *18*, 683.
9. Yeh, I.; von Deimling, A.; Bastian, B. C. *J. Natl. Cancer Inst.* **2013**, *105*, 917.
10. Ren, L.; Wenglowky, S.; Miknis, G.; Rast, B.; Buckmelter, A. J.; Ely, R. J.; Schlachter, S.; Laird, E. R.; Randolph, N.; Callejo, M. *Bioorg. Med. Chem. Lett.* **2011**, *21*, 1243.
11. Gorden, A.; Osman, I.; Gai, W.; He, D.; Huang, W.; Davidson, A.; Houghton, A. N.; Busam, K.; Polsky, D. *Cancer research* **2003**, *63*, 3955.
12. Luo, C.; Xie, P.; Marmorstein, R. *J. Med. Chem.* **2008**, *51*, 6121.
13. Würth, R.; Thellung, S.; Bajetto, A.; Mazzanti, M.; Florio, T.; Barbieri, F. *Drug Discov. Today* **2015**.
14. Dienstmann, R.; Tabernero, J. *Curr. Med. Chem. Anticancer Agents* **2011**, *11*, 285.
15. Finn, L.; Markovic, S. N.; Joseph, R. W. *BMC Med.* **2012**, *10*, 1.
16. Bollag, G.; Tsai, J.; Zhang, J.; Zhang, C.; Ibrahim, P.; Nolop, K.; Hirth, P. *Nat. Rev. Drug. Discov.* **2012**, *11*, 873.
17. Zhan, Y.; Dahabieh, M. S.; Rajakumar, A.; Dobocan, M. C.; M'Boutchou, M.-N.; Goncalves, C.; Pettersson, F.; Topisirovic, I.; van Kempen, L.; del Rincón, S. V. *J. Invest. Dermatol.* **2015**, *135*, 1368.
18. Liu, F.; Cao, J.; Wu, J.; Sullivan, K.; Shen, J.; Ryu, B.; Xu, Z.; Wei, W.; Cui, R. *J. Invest. Dermatol.* **2013**, *133*, 2041.
19. Martinez-Garcia, M.; Banerji, U.; Albanell, J.; Bahleda, R.; Dolly, S.; Kraeber-Bodéré, F.; Rojo, F.; Routier, E.; Guarín, E.; Xu, Z.-X. *Clin. Cancer Res.* **2012**, *18*, 4806.
20. Chapman, P. B.; Hauschild, A.; Robert, C.; Haanen, J. B.; Ascierto, P.; Larkin, J.; Dummer, R.; Garbe, C.; Testori, A.; Maio, M. *N. Engl. J. Med.* **2011**, *364*, 2507.
21. Helvind, N. M.; Hölmich, L. R.; Smith, S.; Glud, M.; Andersen, K. K.; Dalton, S. O.; Drzewiecki, K. T. *JAMA Dermatol.* **2015**, *151*, 1087.
22. Barbaric, J.; Sekerija, M.; Agius, D.; Coza, D.; Dimitrova, N.; Demetriou, A.; Diba, C. S.; Eser, S.; Gavric, Z.; Primic-Zakelj, M. *Eur. J. Cancer* **2016**, *55*, 47.
23. Schmidt, T.; Bergner, A.; Schwede, T. *Drug Discov. Today* **2014**, *19*, 890.

## Figure Captions

**Table 1.** Structures of compounds **3a-3n**.

**Table 2** *In vitro* inhibitory effects of compounds **3 (3a-3n)** against human tumor cell lines, normal cell line.

**Table 3.** Inhibition activity of all tested compounds against BRAF<sup>V600E</sup>.

**Fig. 1.** Chemical structures of known BRAF<sup>V600E</sup> inhibitors and designed structures.

**Fig. 2.** Crystal structure diagram of compound **3f**.

**Fig. 3.** Annexin V-FITC/PI dual-immuno-fluorescence staining after treatment with different concentrations of **31** on WM266-4 cells revealed significantly increased number of apoptotic cells. (A) The apoptosis rate of WM266-4 cells treated with 0, 2, 4 and 8  $\mu\text{M}$  **31** for 24 h. (B) The percentage of apoptotic cells were calculated after the treatment of **31**. Images are representative of three independent experiments.

**Fig. 4.** Annexin V-FITC/PI dual-immuno-fluorescence staining after treatment with different concentrations of **31** on WM1361 cells revealed significantly increased number of apoptotic cells. (A) The apoptosis rate of WM1361 cells treated with 0, 20, 40 and 60  $\mu\text{M}$  **31** for 24 h. (B) The percentage of apoptotic cells were calculated after the treatment of **31**. Images are representative of three independent experiments.

**Fig. 5.** The gel electrophoresis image obtained after DNA fragmentation assay for apoptosis detection. WM266-4 cells were cultured at 37 °C for 24 h in the presence or absence of the various concentrations of compound **31**. DNA was isolated and visualized on a 2.0% agarose gel. From left lanes are: Lane M: Marker (2000bp); Lane 1: 8  $\mu\text{M}$ ; Lane 2: 4  $\mu\text{M}$ ; Lane 3: 2  $\mu\text{M}$ ; Lane 4: 0  $\mu\text{M}$  (CON); Lane M: Marker (15000bp).

**Fig. 6.** Effect of compound **31** on the cell cycle distribution of WM266-4 cells in a dose-dependent manner (0, 2, 4 and 8  $\mu\text{M}$ ). Images are representative of three independent experiments. (G1 phase, green; S phase, yellow and G2/M phase, blue).

**Fig. 7.** Effect of compound **31** on the cell cycle distribution of WM266-4 cells in a time-dependent manner (0, 12, 24 and 36 h). Images are representative of three independent experiments. (G1 phase, green; S phase, yellow and G2/M phase, blue).

**Fig. 8.** Binding mode of compound **31** with BRAF<sup>V600E</sup> (PDB code: 2FB8). (A) 2D diagram of the interaction between compound **31** and amino acid residues of the nearby active site. (B) 3D diagram of compound **31** inserted in the BRAF<sup>V600E</sup> binding site: for clarity, only interacting residues are displayed.

**Scheme 1<sup>a</sup>.**

# Design, synthesis and biological evaluation of novel Benzo- $\alpha$ -pyrone containing piperazine derivatives as potential BRAF<sup>V600E</sup> inhibitors

Long-Wang Chen<sup>a†</sup>, Ze-Feng Wang<sup>a†</sup>, Bo Zhu<sup>b</sup>, Ruo-Jun Man<sup>a</sup>, Yan-Dong Liu<sup>a</sup>, Yuan-Heng Zhang<sup>a</sup>, Bao-Zhong Wang<sup>a\*</sup>, Zhong-Chang Wang<sup>a\*</sup>, Hai-Liang Zhu<sup>a\*</sup>

<sup>a</sup> State Key Laboratory of Pharmaceutical Biotechnology, Nanjing University,

Nanjing 210023, People's Republic of China

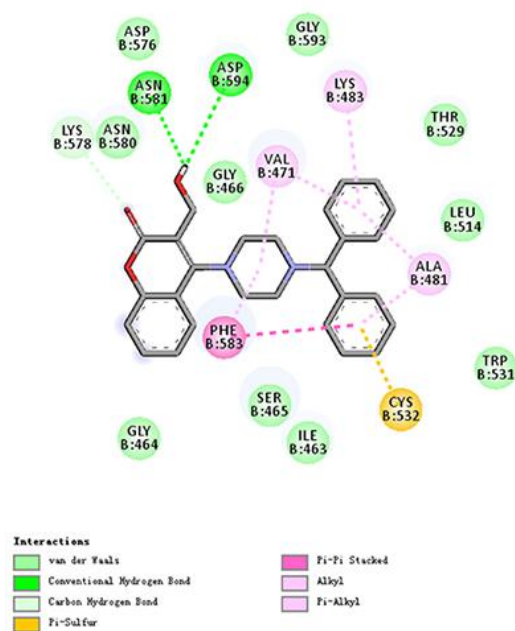
<sup>b</sup> Jiangsu Chia Tai Tianqing Pharmaceutical Co., Ltd. Nanjing 210000, P. R. China

\*Corresponding author. Tel. & fax: +86-25-89682572;

E-mail: [zhuhl@nju.edu.cn](mailto:zhuhl@nju.edu.cn)

<sup>†</sup>These two authors equally contributed to this paper.





Virtual screening and scaffold growth were combined together to achieve a series of novel compounds (**3a-3n**) bearing the benzo- $\alpha$ -pyrone scaffold. Among them, compound **3l** showed most powerful antiproliferative activity ( $IC_{50} = 2.24 \mu M$  for A375 and  $IC_{50} = 1.35 \mu M$  for WM266-4) and enzyme inhibition activity ( $IC_{50} = 0.37 \mu M$ ). **3l** could effectively cause melanoma cells apoptosis in a dose-dependent manner, significantly induce DNA fragmentation and arrest cell cycle at the G0/G1 phase. Docking simulation was performed to explore the binding model of compound **3l** with BRAF<sup>V600E</sup>.